

## Study of Low-Dose-Rate Radiation Effects on Commercial Linear Bipolar ICs

R.K. Freitag and D.B. Brown

Naval Research Laboratory  
Washington, DC 20375

### Abstract

The results of a detailed study of the degradation of commercial linear bipolar ICs due to irradiation at four dose rates are presented. The time dependence of the degradation rate at the different dose rates is shown to be consistent with a model that describes a mechanism for defect generation in the devices used in this study. Based on this model, an accelerated test procedure for bipolar devices is proposed.

### I. INTRODUCTION

Many linear bipolar ICs have been shown to suffer greater degradation when exposed to ionizing radiation at a low dose rate than at higher dose rates typical of laboratory sources [1-4]. These effects are generally believed to be due to the enhanced degradation of the bipolar transistors in the circuit. One effect of irradiation on a bipolar transistor is to increase the base current. This increase is thought to be due to the generation of defects in the oxide covering the emitter-base junction. The circuits used in this work have PNP input transistors, and we assume the change of the input bias current of the IC reflects the change in the base current of this transistor.

We will show that the enhanced low dose rate degradation effects observed in the devices studied in this work cannot be fully explained using the simple form of time dependent effects (TDE) which has been successful in treating MOS devices. A consequence of this is that the accelerated test methods often used for MOS devices are inadequate for bipolar devices that degrade much more severely at lower dose rates than at higher dose rates. In particular, the net result of a high dose rate irradiation followed by an anneal often does not simulate the effects obtained during a low dose rate exposure [5]. It will be shown that the enhanced low dose rate sensitivity of these devices can be explained by a model that assumes that the defect responsible for the degradation results from the interaction of two reactant species generated by the radiation. By considering the generation, transport, and interaction of these two reactants, we construct a model that is consistent with the observed time dependence of the degradation process. An essential part of this model is that the interaction of these two species can be characterized using binary reaction rate theory.

A major result of this work is the demonstration that the effect of an increment of radiation on these devices is not, in general, independent of previous increments of irradiation, consistent with the fact that the simple form of TDE cannot explain the results. To explain this, we assume that one of the

two reactant species is generated at some distance from the region in the oxide where the interaction with the second reactant may occur. This first reactant is assumed to slowly transport to the region in the oxide where it can interact with the second radiation-induced reactant to generate the defect responsible for the increase in the input bias current. The rate of this defect formation is proportional to the concentrations of these two reactants near the sensitive Si-SiO<sub>2</sub> interface. It will be shown that this transport of a reactant species is consistent with the radiation response of the devices studied during and after irradiation at four dose rates. Using this model we suggest that, for the devices described in this work, irradiations which take longer than this transport time produce enhanced damage as compared to irradiations which take less than this time. We use our model and data to suggest an accelerated test method for hardness assurance testing of devices intended for space applications.

### II. EXPERIMENTAL DETAILS

The devices used in this study were commercial versions of the LM111 comparator and the LM158 operational amplifier, both manufactured by National Semiconductor. All devices of each type are from the same date code. Irradiations were carried out using a small Cu-target x-ray source, and dosimetry was performed using a calibrated, commercial PIN dosimeter. All doses stated are in units of rd(Si). The irradiations were performed at room temperature with all leads shorted. The dose rates employed were 50, 1, 0.3, and 0.1 rd(Si)/s.

As a measure of the damage to the devices, we have monitored the change of the input bias current during and after irradiation. Both of these circuits employ substrate PNP input transistors. We assume that the radiation generates defects in the oxide layer over the emitter-base junction of these transistors, and it is these defects that are responsible for the increase of the input bias current. In this paper we present the change of  $I_B^+$ . We have also measured  $I_B^-$  and the results are similar. All measurements were made approximately one minute after each exposure. The annealing behavior (with all leads shorted) following the completion of the irradiation was also monitored.

### III. EXPERIMENTAL RESULTS

The results of the irradiations of the LM111 at four dose rates are shown in Fig. 1 which shows the change of the input bias current ( $\Delta I_B$ ) as a function of total dose. As expected, for a given total dose, the damage per unit dose is clearly enhanced as the dose rate is decreased. Note, however, that the

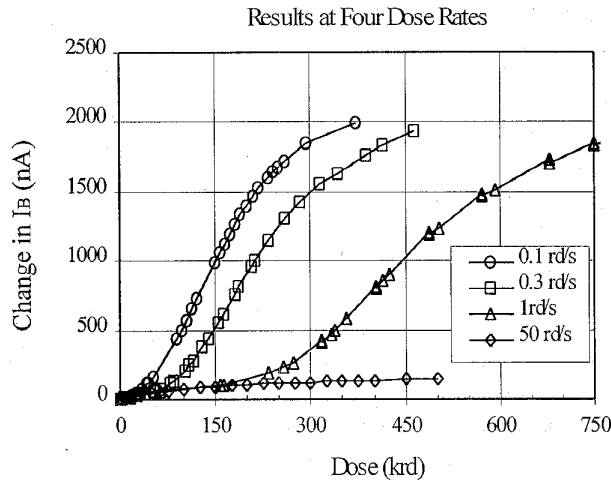


**Figure 1:** The change in the input bias current of the LM111 due to irradiation at four dose rates.

ratio of the  $\Delta I_B$  at one dose rate to the  $\Delta I_B$  at another dose rate, for a given total dose, is not constant. At low total doses the change in  $I_B$  is similar (within a factor of 2) for all the dose rates studied. As the total dose is increased, the ratio of the degradation generated during the lower dose rate exposures to that generated at a higher dose rate depends on the total dose. For example, compare the results during the irradiation at 1 rd/s to the results of the irradiation at 50 rd/s. After exposure to the first 150 krad, the irradiation at either dose rate generates approximately the same change in  $I_B$ . After a 450 krad exposure, however, the irradiation at 1 rd/s results in a shift of  $I_B$  that is approximately 5 times greater than that due to the irradiation at 50 rd/s. A similar dependence on total dose can be seen in the results reported by Johnston et al. [4], Emily [5], Cole et al. [6], and Bonora et al. [7]. This dependence of the relative degradation at the different dose rates on total dose needs to be addressed by any model used to describe the defect generation mechanism in these circuits.

To better illustrate the mechanism(s) responsible for the observed dose rate effects, it is useful to study the rate at which the devices degrade at the different dose rates. Figure 2 shows the damage rate (nA/krad) vs. dose corresponding to the data shown in Fig. 1. That is, Fig. 2 is a plot of the first derivative of the data shown in Fig. 1. At low total doses the shifts per krad are all within a factor two of each other for all four dose rates. However, at higher total doses, there occurs a dramatic increase in the degradation rate for the exposures at 0.1, 0.3 and 1 rd/s, but not the 50 rd/s case which decreases monotonically with increasing dose. Note also, that the dose at which the damage rate begins to increase is very different for the three lower dose rates. The onset of the increase in the degradation rate occurs at a progressively lower accumulated dose as the dose rate is decreased. The observed large increase in the damage rate is followed by a decrease at higher doses (for the lower dose rates). This decrease reflects the saturation in the

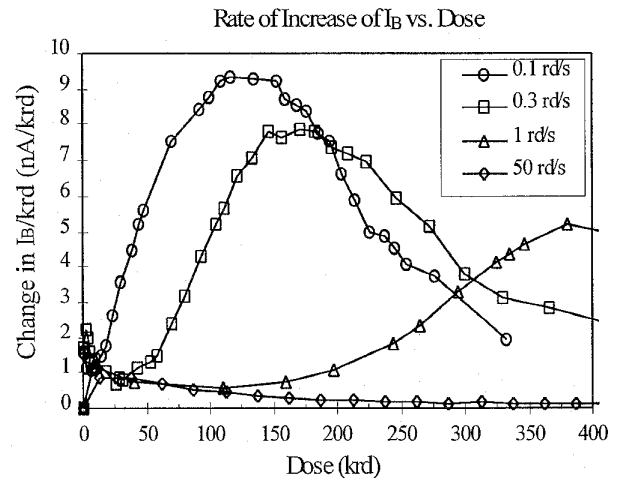


**Figure 2:** First derivative of the change in  $I_B$  (with respect to dose) as a function of total dose. For a more detailed view at the lower doses, see Fig. 10.

degradation that occurs in these devices at a  $\Delta I_B$  of about 2000 nA.

It is very instructive to replot the degradation rate data (nA/krad) shown in Fig. 2 as a function of irradiation time rather than total dose. This is shown in Fig. 3. Plotted as a function of time, the effect of the radiation for the three lower dose rates look quite similar. At short times, the damage rate first increases, then decreases until about 100,000 seconds after the start of the irradiation (see Fig. 10 for a blowup of this time regime). At the three lower dose rates the damage rate begins to increase at about 100,000 seconds, and then continues to increase steadily for several hundred thousand seconds. The reason that a similar increase in the damage rate is not seen during the irradiation at 50 rd/s is because the irradiation (to a

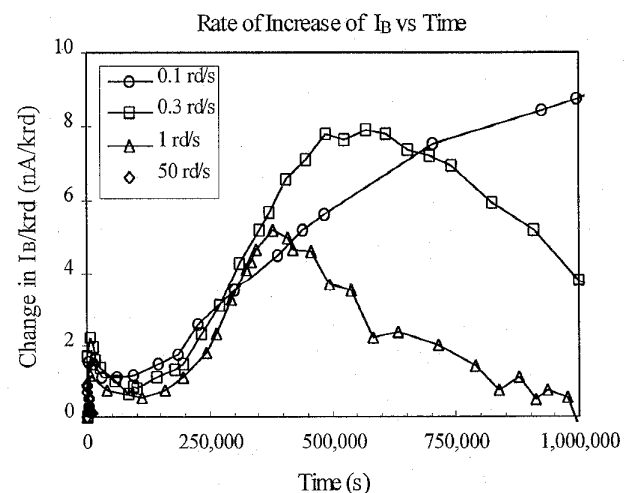


**Figure 3:** First derivative of the change in  $I_B$  (with respect to dose) as a function of irradiation time.

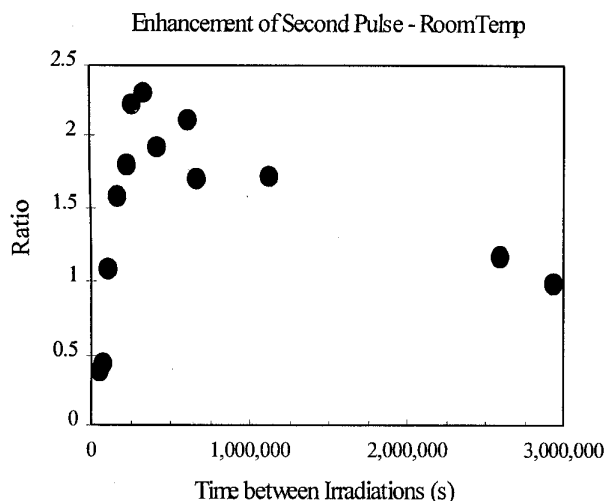


**Figure 4:** The ratio of the degradation due to the second irradiation to the degradation due to the first irradiation as a function of time between irradiations at room temperature.

total dose of 500 krd) is completed in significantly less time (10,000 s).

One might question whether the increase in the damage rate observed during the lower dose rate irradiations as shown in Figs. 2 and 3 would occur if the 50 rd/s irradiation were continued for a sufficiently long time. Since the device would probably become non-functional if the 50 rd/s irradiation were continued for this long, consider the following procedure. Irradiate a device at 50 rd/s in two equal exposures with a variable time interval between the irradiations. Then compare the degradation that occurs during the second exposure to the degradation generated during the first exposure. The results of this procedure are shown in Fig. 4, which shows the ratio of the  $\Delta I_B$  due to the second irradiation to the  $\Delta I_B$  due to the first irradiation as a function of the time interval between the two irradiations (each irradiation to 150 krd). Clearly, the ratio of the degradation that occurs during the second irradiation to that of the first irradiation is not a constant. The amount of degradation that occurs during the second irradiation to 150 krd depends on the time interval between the two irradiations. For "short" time intervals the ratio is less than 1, corresponding to less damage per krad during the second irradiation. As the time interval is increased, the ratio of the damage due to the two irradiations increases. Note that the increase in the ratio begins at about 100,000 s and reaches a maximum at about 400,000 seconds for this set of devices. This result is consistent with the data shown in Fig. 3 for the lower dose rate irradiations which shows the degradation rate beginning to increase after about 100,000 seconds and continuing to increase for several hundred thousand seconds.

The data in Fig. 3 showing the steady-state low dose rate results and the data in Fig. 4 showing the results of incremental irradiations at 50 rd/s both show an enhancement of the damage rate that begins about  $10^5$  seconds after the start of the

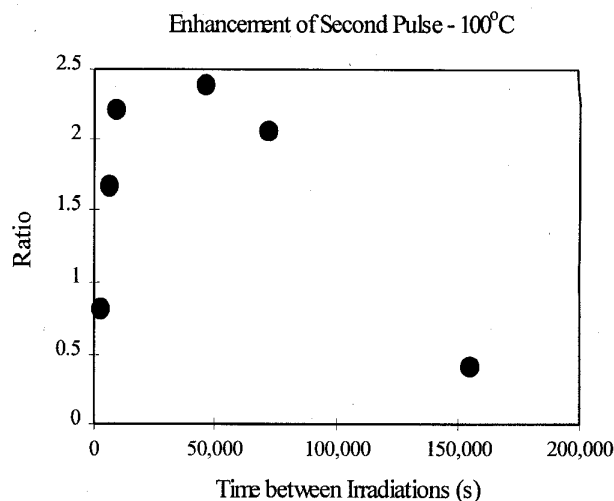


**Figure 5:** The ratio of the degradation due to the second irradiation to the degradation due to the first irradiation as a function of time between irradiations at 100°C.

irradiation. This is consistent with the motion of a radiation-induced species with a transport time on the order of  $10^5$  seconds at room temperature. A second two-pulse experiment, similar to the one just described, was performed where the devices were heated to 100°C during the time intervals between each pair of room temperature irradiations at 50 rd/s. The results of this experiment are shown in Fig. 5. Qualitatively, these results are similar to the room temperature results shown in Fig. 4. However, the time scale is decreased by about an order of magnitude. This decrease in the time interval is consistent with the transport being a thermally activated process.

Further evidence in support of the motion of an active species can be seen in the post-irradiation behavior shown in

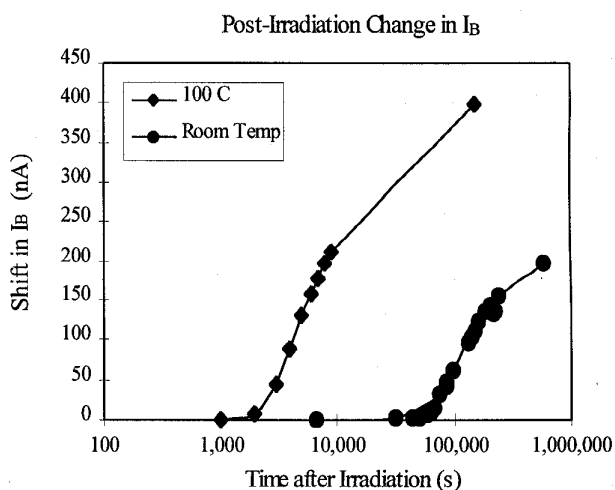


**Figure 6:** Post-irradiation degradation at room temperature and 100°C. Both results are following a 150 krad irradiation at room temperature.

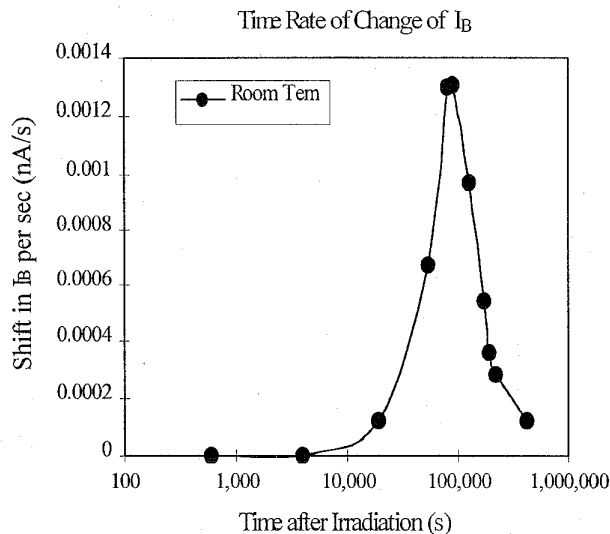


**Figure 7:** Time rate of change (nA/s) during room temperature anneal following a 150 krd irradiation.

Fig. 6, which shows the post-irradiation response of  $I_B$  following a 150 krd room temperature irradiation at 50 rd/s. Results at both room temperature and 100°C are shown. In both cases, there is little or no change of the input bias current immediately following the irradiation. At room temperature there is a delay of about 50,000 seconds before an increase of  $I_B$  is observed. At 100°C, this time interval before a change in  $I_B$  is observed is reduced to about 3000 seconds. This temperature dependence is consistent with the results of the two-pulse experiments discussed earlier. Figure 7 shows the slope (in nA/s) of the room temperature data shown in Fig. 6 plotted vs. time. Note

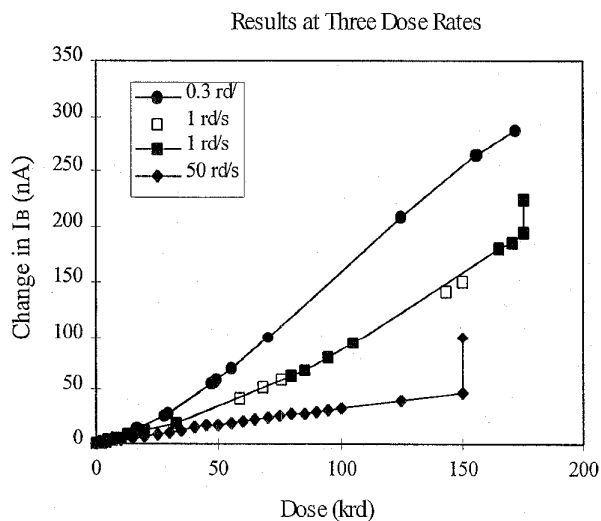


**Figure 8:** The change in input bias current of the LM158 at three dose rates. the vertical line segments represent the results of approximately 5 day room temperature anneals.

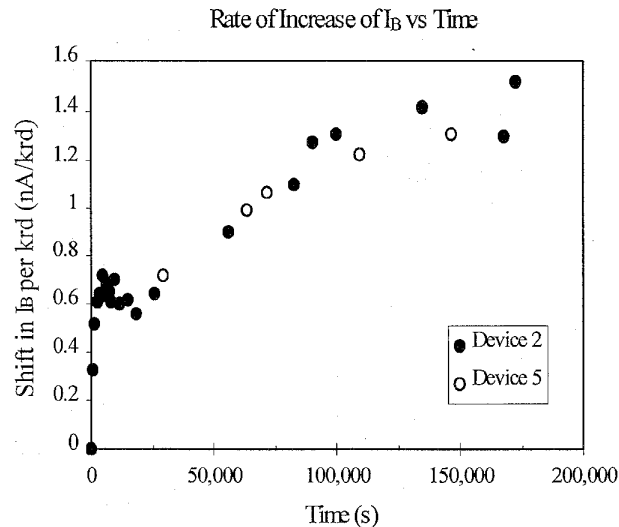


**Figure 9:** Results showing the damage rate (nA/krd) vs. time for the commercial version of the LM158.

that after an initial time of very small change in  $I_B$ , there is a sharp increase in the rate of change after about 50,000 s, and a maximum occurs after about 100,000 s. After this maximum is reached, the rate of change of  $I_B$  decreases steadily and seems to be approaching zero at very long times. The significance of this will be treated in the Discussion section.

Experiments have also been performed on a commercial version of the LM158 at 50, 1, and 0.3 rd/s. An enhanced low dose rate sensitivity is also observed for this set of devices as shown in Fig. 8. Again, we find that the damage rate depends on the total dose (compare the results at 25 krd to that at 125 krd). A plot of the damage rate vs. time for these devices is shown in Fig. 9 for an irradiation at 1 rd/s. Note the rise-fall-rise pattern similar to the results shown in Figs. 2 and 3 for the LM111. Although the time before the second increase in the damage rate is less than that for the LM111, the results are qualitatively similar to the radiation response of the LM111. Previous results of a two-pulse experiment using the commercial version of the LM158 also show a time dependent response during the second irradiation, similar to that observed for the LM111 [8]. Note also in Fig. 8 that the combined effect of an irradiation at 50 rd/s plus an anneal for several days (approximately 400,000 s) does not result in the same change of input bias current as results from an irradiation at either of the two lower dose rates shown.

#### IV. DISCUSSION (MODEL)

There are several important points to emphasize about the data shown above. First, the ratio of the degradation due to an exposure at one dose rate to that of another dose rate may depend on the total dose. Second, the degradation rate during an irradiation depends on previous exposures the device may have been subjected to in a way that is not simply additive. For

example, the results of the two-pulse experiments would be quite different if the radiation effects were additive (see Figs. 4 and 5). Third, there appears to be a characteristic time after which the degradation rate increases dramatically that is similar for all dose rates considered (see Fig. 3).

We have constructed a model that describes a mechanism that is consistent with the results shown above. Implicit in this model is that the radiation generates a defect located at or near the Si-SiO<sub>2</sub> interface on top of the emitter-base junction of the (substrate PNP) input transistor. It is this defect that is responsible for the increase in the input bias current. The model assumes that this defect is generated by the interaction of two radiation-induced species which we call "A" and "B", and that the rate of defect formation (as measured by  $\Delta I_B$ ) can be described by binary reaction rate theory.

The essence of the model is as follows: The model treats the interaction of two reactant species, "A" and "B", and assumes that the defect generation rate is proportional to the product of the concentrations of these two at or near the Si-SiO<sub>2</sub> interface. At early times during the irradiation the radiation generated reactant "A" combines with a pre-existing quantity of reactant "B", generating the defects that are responsible for the measured increase in  $I_B$ . The rate of this reaction determines the damage rate at "early" times during the irradiation. After an initial increase in the damage rate (resulting from the increase in the concentration of "A" generated by the irradiation), the reaction continues at a decreasing rate as the pre-existing reactant "B" is consumed by the radiation induced "A". This is consistent with the data in Figs. 2 and 3 showing the results of the LM111 and Fig. 9 showing results for the LM158. That is, for the lower dose rate irradiations there is an initial increase at short times (on the order of thousands of seconds), which is then followed by an interval where the degradation rate decreases before starting to increase after about 100,000 seconds. During the 50 rd/s irradiation, it is seen in Fig. 2 that an early increase in the damage rate is followed by a monotonic decrease up to 500 krd. This corresponds to only 10,000 seconds and thus the second increase that is seen at lower dose rates does not occur.

We now make a key assumption. We assume there is secondary source of reactant "B". This secondary "B" is generated during the irradiation at a location some distance from the critical Si-SiO<sub>2</sub> interface. The "B" produced at this secondary source then migrates to the sensitive interface where it can react with the species "A" generated near that interface during the irradiation to form additional defects. This results in an increased reaction rate due to the arrival of the secondary "B" if the irradiation is taking place during this time. This is reflected in the sharp increase in the degradation rate that is observed (Figs. 3 and 9) after a significant time into the irradiation. From Figs. 3 and 9, we can estimate a transport time of about 100,000 seconds for the LM111's, and about 50,000 seconds for the LM158's used in this work.

Further support for the model can be seen in Figs. 4 and 5. During the first irradiation the defect generation rate is largely determined by the rate of the reaction of species "A" generated during the irradiation with pre-existing species "B".

During the second irradiation following a sufficiently long time interval, the generation rate is determined by the reaction rate of species "A" with both the remaining concentration of pre-existing "B" and the concentration of secondary "B" produced during the first irradiation. This secondary "B" is generated during the first irradiation and subsequently migrates to the sensitive interface. A transport time of about 10<sup>5</sup> s for this secondary "B" is consistent with the room temperature results shown in Fig. 4. Figure 5 shows that the transport time of species "B" is significantly reduced as the temperature is raised, consistent with a thermally activated process. Based on these results and the annealing data shown in Fig. 6, a rough estimate of the activation energy is about 0.37 eV. Note also in Figs. 4 and 5 that for short time intervals between the irradiations, the ratio of the degradation due to the second irradiation to degradation due to the first irradiation is less than one. That is, the damage generated during the second irradiation is less than the first irradiation, which is consistent with little or no secondary "B" arriving during this time.

Additional evidence in support of the model is supplied by the annealing data shown in Fig. 6. Consider the room temperature data. Immediately following the end of the irradiation, there is very little change in  $I_B$ . This is followed by a large increase in  $I_B$  starting about 50,000 seconds after the end of the irradiation. This is consistent with the delayed arrival of the secondary "B" generated during the irradiation where it can react with the species "A" generated during the irradiation. At later times the rate of increase of  $I_B$  decreases, as shown in Fig. 7. That is, the defect generation rate decreases at long times. A possible explanation for this fall-off is that since species "A" is no longer being produced, because the irradiation has ended, the concentration of "A" is being decreased by the reaction with "B" as it arrives at the interface. As the concentration of "A" decreases the rate of defect generation decreases.

To this point we have relied on the assumption that the observed enhanced effect at lower dose rates can be explained by the slow transport of species "B". Qualitatively, this effect is very similar to that described by others in studies of latent interface trap generation [9-11] and the delayed increase in 1/f noise in pMOS transistors [11]. In the paper by Fleetwood et al. [11] it is suggested that the retarded transport of hydrogen is a likely candidate responsible for the post-irradiation build-up of interface traps, the delayed increase in 1/f noise in pMOS structures, and the enhanced low dose rate effects in bipolar devices.

Comparing the post-irradiation behavior presented by Fleetwood et al. [11] with the results presented above adds additional support for the argument that latent interface trap buildup, enhanced 1/f noise at long times, and low dose rate effects in bipolar devices result from a similar physical process. For example, in the paper by Fleetwood et al. [11], it is reported that the time before the onset of the increase in 1/f noise and the increase in the number of interface traps is on the order of 10<sup>5</sup> seconds, and this time is greatly reduced at elevated temperatures. Also, an estimate of the activation energy for the process involved in latent interface trap buildup in MOS devices is

reported as 0.47 eV [10], which compares favorably with the rough estimate obtained for the devices used in this work (approximately 0.37 eV).

It will be shown below that the proposed model is very consistent with the experimental results presented above for the LM111. These devices use a PNP input transistor, and we assume that the measured degradation reflects the damage induced in this transistor. Whether this model is also applicable to NPN devices is not known. It should be emphasized, however, that the similar time dependence of the defect generation process that is reported in this work (bipolar structures) and the work on the generation of latent interface traps and increased 1/f noise (both in MOS structures) reported by Fleetwood et al. [11] suggests that a common physical process is responsible for the defect generation, and that this process is likely to also occur in NPN structures. For the devices used in this work, it appears that it is the defects generated after the transport of secondary "B" that are predominantly responsible for the enhanced degradation observed at low dose rates. We can speculate that the same process also occurs in NPN devices, but the degree to which this defect affects the electrical performance of the device is uncertain. Further work is needed to resolve this question.

## V. APPLICATION OF THE MODEL

To make the model more quantitative, we assume that the defect generation rate can be quantified by time rate of change of the input bias current ( $dI_B/dt$ ). We further assume that the defect generation rate can be described using binary reaction rate theory characterized by the following equations:

$$\frac{dI_B}{dt} = X k n_A n_B \quad (1)$$

$$\frac{dn_A}{dt} \approx -k n_A n_B + Y D \quad (2)$$

$$\frac{dn_B}{dt} = -k n_A n_B + [\text{delayed source}] \quad (3)$$

where  $I_B$  is the input bias current,  $X$ ,  $Y$ , and  $k$  are physical parameters,  $n_A$  and  $n_B$  are the densities of "A" and "B" at or near the Si-SiO<sub>2</sub> the interface, and  $D$  is the dose. For further details of these quantities see the Appendix.

We have obtained approximate analytical solutions to the reaction rate equations appropriate to short times (less than 100,000 sec) and to long times (greater than 100,000 sec). For details of the assumptions made to obtain these results see the appendix. For short times, it can be shown that an approximate solution to the rate equations is:

$$\frac{dI_B}{dt} = A \left[ 1 - \exp\left(-\frac{D}{k_1 D}\right) \right] \exp\left(-\frac{D}{k_2}\right) \left[ 1 + \frac{1}{2} \frac{k_3 D^2}{k_1 k_2 D} \right] \quad (4)$$

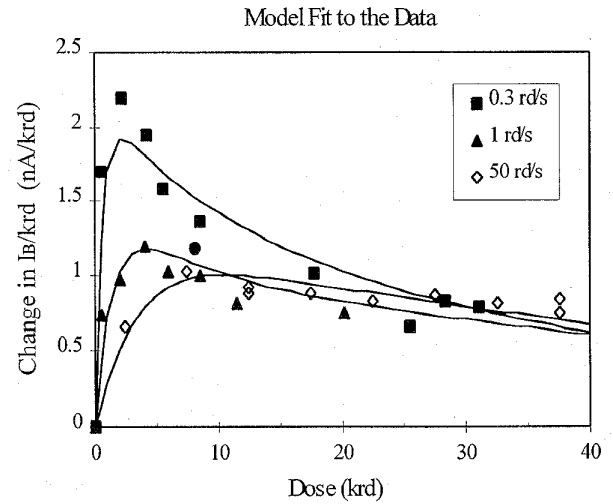


Figure 10: Plot of the model fit (lines) for "short times", and the experimental data (symbols) for the LM111.

Figure 10 shows a plot of this equation as lines and the experimental data for the LM111 as symbols for three dose rates. The calculated curves provide a reasonable fit to the data. In particular, both the calculated curves and the data show the change of the reaction rate with increasing dose that is caused first by an increasing concentration of "A" that is generated by the radiation. This is followed by a subsequent decrease in the reaction rate due to the decreasing concentration of reactant "B" as it reacts with the radiation-induced "A" to form the defect responsible for the increased bias current.

Table 1 shows the parameters that were used to fit Eqn. 4 to the experimental data as shown in Fig. 10. Note, first, that we have used average dose rates (25, 0.9 and 0.3 rd/s) in place of the irradiation dose rates (50, 1 and 0.3 rd/s) in order to approximately account for the fact that dose rate was zero during a significant measurement time. Second, it will be noted that it was found necessary to use a different set of the parameters  $A$ ,  $k_1$ , and  $k_3$  for each of the three sets of experimental data. We suggest two possible explanations for the necessity to vary these parameters. One possibility is that the quantities of the reactants available to produce the change in  $I_B$  may be a function of the dose rate. Fleetwood et al. have previously suggested that this

Table 1: Table of constants for Eqn. 4.

Avg. Dose Rate (rd/s)	A (nA/krd)	$k_1$ (s)	$k_2$ (rd)	$k_3$ (unitless)
25	1.7	200	20000	0.24
.9	1.5	1600	20000	0.07
0.3	2.2	2000	20000	0.016

could be caused by space charge effects [13]. A second possibility is that inaccurate approximations were made in obtaining an analytic solution of the differential equations. See the appendices for additional discussion of this possibility.

For "long" times an approximate solution to the rate equations is:

$$\frac{dI_B}{dt} = C \left[ 1 - \exp\left(-\frac{(D/\bar{D})-t_d}{k_2}\right) \right] \quad (5)$$

This equation (lines) and the experimental data (symbols) are plotted in Fig. 11. Again, the calculated curve is a reasonable fit to the data. In particular, this solution agrees well with the total dose at which each data set begins to show an increase in the damage rate. We reiterate that Eqn. 5 is not intended to describe the defect generation at short times. For the short time regime see Eqn. 4. Further, as previously stated, the decrease in the generation rate at higher total doses is due to a saturation effect which we did not model. The model fits shown in Fig. 11 were obtained using the fit parameters  $C=9.2$  nA/krd,  $k_2=200,000$  s, and  $t_d=170,000$  s.

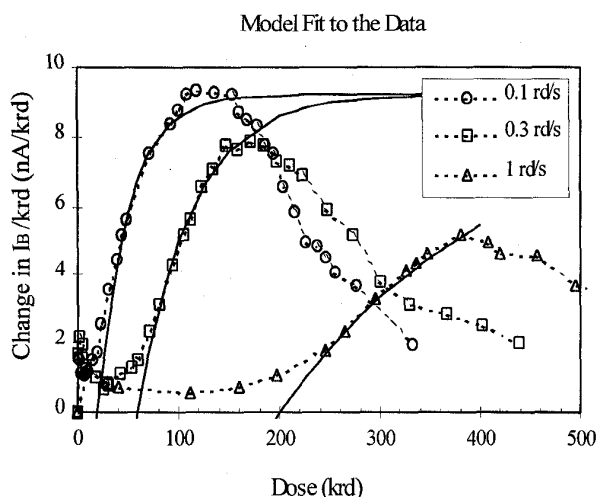


Figure 11: Plot of the model fit (lines) for "long times", and the experimental data (symbols) for the LM111.

## VI. IMPLICATIONS FOR HARDNESS ASSURANCE.

It has been demonstrated that standard hardness assurance testing methods commonly used for MOS devices yield non-conservative results when applied to bipolar devices. That is, the standard methods employing irradiation at laboratory dose rates and anneal often do not generate the same degradation as a low dose rate irradiation [1,2,12]. More recently, it has been shown that a combination of high temperature irradiations at a high dose rate and otest can be used to bound the damage that occurs at low dose rates with reasonable success [13-17]. Both of these testing techniques are derived from models of the basic mechanisms of defect generation that are inadequate to explain the results presented above. In particular, the two-pulse

experiments, as well as the rise-fall-rise pattern of the degradation rate shown in Figs. 3 and 9, are not readily explained by the models used.

An important implication of the results and the model discussed above is that any hardness assurance test methodology should consider the relatively slow transport of species "B". That is, the defect generation mechanism that results in the measured device degradation is enhanced by the delayed arrival of an additional quantity of reactant "B". If the irradiation is continued for times long enough for the reactant "B" to arrive, then the degradation rate will increase. For the devices used in this work it is seen that this transport time can be as long as  $10^5$  seconds after the start of the irradiation (at room temperature). Thus irradiations taking longer than this time will result in enhanced degradation compared to irradiations taking much less time.

We have shown that the transport of reactant "B" is greatly accelerated at  $100^\circ\text{C}$ . It may be possible to use this effect to develop an accelerated test for total dose effects at low dose rates. A possible protocol for a hardness assurance test to a given total dose is as follows. Expose a device at room temperature to half the specified total dose at a typical laboratory dose rate. Following this irradiation, let the device anneal at  $100^\circ\text{C}$  for several hours. Next, re-irradiate the device until the total accumulated dose is as specified. Then, follow this second irradiation with a second anneal at  $100^\circ\text{C}$  for several hours.

A preliminary test of this methodology has been performed where the device was irradiated at 50 rd/s to a total dose of 150 krd in two increments separated by an intermediate anneal at  $100^\circ\text{C}$  for three hours. After completion of the second irradiation, the device was annealed again at  $100^\circ\text{C}$  for 4.4 hours. The net degradation following this procedure was 7.4 times greater than the degradation generation by a room temperature irradiation at 50 rd/s to the same total dose. The enhancement factor of 7.4 observed in this accelerated test is somewhat larger than the enhancement that has been reported in other work on similar devices using very low dose rate irradiation. See, for example, the data presented by Johnston et al. [3], where an enhancement factor of approximately 4.8 was found when comparing the effect resulting from an irradiation at 0.002 rd/s to the effect of an irradiation at 50 rd/s.

Further work is needed to determine the optimal experimental conditions for using this approach. That is, the optimal temperature and duration of the intermediate anneal needs to be determined. Although it seems likely that the mechanism described above is a major source of the enhanced low dose rate sensitivity of the devices used in this work, further study is required to determine whether this is the case for other devices.

## VII. SUMMARY AND CONCLUSIONS

We have presented data that illustrates several important features of the defect generation mechanism in the devices studied. First, the degradation generated per unit dose is both dose rate and total dose dependent. Second, the magnitude of the effects of an irradiation depends on previous irradiations, and this is not explainable by simple time dependent effects. That is,

the results are not simply additive. Third, and most important, is that there appears to be a characteristic time that can be associated with the onset of enhanced degradation.

We have shown that the defect production rate described by the model presented above defines two time regimes. At relatively short times (typical of high dose rate exposure), the defect generation rate is dominated by the interaction of the radiation-induced concentration of species "A" with the pre-existing concentration of species "B" near the sensitive Si-SiO<sub>2</sub>. For sufficiently long irradiations (typical of low dose rate exposure), the defect production rate is enhanced by the arrival of a secondary source of species "B" that has been generated by previous radiation exposure. It is this secondary source of "B" that is mainly responsible for enhanced low dose rate sensitivity of these devices. A consequence of this model is that it is possible to use our understanding of this effect to devise a hardness assurance test method for space applications.

## VIII. APPENDIX

### A. Initial Stage

This, and the following sections present a brief derivation of equations used in the main body of this paper. See the body of the paper for the background necessary to understand the motivation of the development presented in these appendices.

We begin by assuming that defect components A and B react to cause a change in the input bias current according to

$$\frac{dI_B}{dt} = X k n_A n_B \quad (\text{A1})$$

where,

- $I_B$  = input bias current in nanoamps
- $t$  = reaction time in seconds
- $n_A$  = atoms/cm<sup>2</sup> of reactant A
- $n_B$  = atoms/cm<sup>2</sup> of reactant B
- $k$  = reaction rate constant
- $X$  = conversion from number of reaction product/cm<sup>2</sup> to shift in  $I_B$  in nanoamps.

We assume that there is an initial concentration of the reactant B,  $n_B^0$ . We further assume that the reactant A is produced by the irradiation so that at short times

$$\frac{dn_A}{dt} \approx -k n_A n_B + Y \dot{D} \quad (\text{A2})$$

In Eqn. A2 the first term represents the consumption of reactant A due to its reaction with B and the second term represents the creation of new reactant A by the radiation. Further,  $\dot{D}$  is the dose rate and  $Y$  is the number increase of A per rad absorbed. It is straightforward to show that for small times where  $n_B \approx n_B^0$  that Eqn. A2 can be solved for  $n_A$ , giving

$$n_A = \frac{Y \dot{D}}{k n_B^0} [1 - \exp(-k n_B^0 t)] \quad (\text{A3})$$

Note that  $n_A$  approaches  $(Y \dot{D})/(k n_B^0)$  as  $t$  increases.

Substituting in Eqn. A1 gives

$$\frac{dI_B}{dt} = X Y \dot{D} [1 - \exp(-k n_B^0 t)] \quad (\text{A4})$$

This is qualitatively what we observe experimentally. That is,  $dI_B/dt$  increases at early times.

### B. Second Stage

In this section we wish to consider the expected behavior for times longer than  $t = 1/(k n_B^0)$ . For this time frame we will assume

$$n_A \approx \frac{Y \dot{D}}{k n_B^0} \quad (\text{B1})$$

and

$$\frac{dn_B}{dt} = -k n_A n_B \quad (\text{B2})$$

With these assumptions it is straightforward to show that

$$n_B = n_B^0 \exp \left[ -t \frac{Y \dot{D}}{n_B^0} \right] \quad (\text{B3})$$

Substituting into Eqn. A1 gives

$$\frac{dI_B}{dt} = X Y \dot{D} \exp \left[ -t \frac{Y \dot{D}}{n_B^0} \right] \quad (\text{B4})$$

This again, is qualitatively what we observe experimentally. In this time regime,  $dI_B/dt$  decreases.

### C. Combination of First and Second Stages

It is a useful approximation to combine the results for the first two stages, giving

$$\frac{dI_B}{dt} = X Y \dot{D} [1 - \exp(-k n_B^0 t)] \exp \left[ -t \frac{Y \dot{D}}{n_B^0} \right] \quad (\text{C1})$$

Although the above equation has the qualitative behavior observed at early times in our experimental data, it may lack quantitative accuracy due to the approximations involved in its derivation. In particular, the assumption in Eqn. B1 ignores a probable slow increase in  $n_A$  which results from the exhaustion of the initial supply of B. One can perform a first order expansion solution to partially correct for this effect, giving

$$\frac{dI_B}{dt} = X Y \dot{D} [1 - \exp(-k n_B^0 t)] \times \exp \left[ -t \frac{Y \dot{D}}{n_B^0} \right] [1 + \frac{1}{2} k Y \dot{D} t^2] \quad (\text{C2})$$



The above results appear to represent a practical limit for a closed-form solution to the differential equations, and after making a few substitutions is equivalent to Eqn. 4 used in the text. Obtaining a numerical solution would be more accurate and should be an interesting extension of this work.

#### D. Third Stage

The equations derived in sections A-C show an initial rise and then a subsequent fall of  $dI_B/dt$ . However, we have experimentally observed a rise-fall-rise pattern. That is, something causes  $dI_B/dt$  to increase in the time range of about 50,000 s to 500,000 s. We hypothesize that this effect is caused by an extra source of reactant B that is generated during the irradiation. This extra B arrives at the reaction site at a delayed time (e.g. 50,000 to 500,000 s). In order to treat this effect, let us set

$$\frac{dn_B}{dt} \approx -k n_A n_B + \int_{t-d}^{t'} \dot{D} f_B(t-t') dt', \quad (D1)$$

where the first term represents the consumption of B by reaction with A, and the second term represents the arrival of new B by the delayed mechanism. In this equation the function  $f_B(t)$  gives the time dependence of the arrival of the delayed B. Eqn. D1 and the remainder of this section are intended to capture the principal effects taking place during the time that the delayed B is arriving at the reaction site.

Let us make the rough approximation that

$$f_B(t) = 0 \quad \text{for } t \leq t_d \quad (D2)$$

and

$$f_B(t) = P \exp\left[-\frac{(t-t_d)}{\tau_4}\right] \quad \text{for } t > t_d \quad (D3)$$

where  $t_d$  is a delay time for the beginning of the arrival of the secondary B,  $\tau_4$  is a characteristic time for the time frame over which the delayed B arrives, and P is a constant that is proportional to the amount of secondary B generated per unit of absorbed radiation. Further, following reasoning similar to that used in the Stage 2 treatment, let us assume that  $n_A$  is roughly given by

$$n_A \approx m \frac{Y \dot{D}}{k n_B^0} \quad (D4)$$

where  $m$  is a constant of the order of one. With the above assumptions, it can be shown that

$$\frac{dn_B}{dt} = k m \frac{Y \dot{D}}{k n_B^0} n_B^0 \dot{D} P \tau_4 \left\{ 1 - \exp\left[-\frac{(t-t_d)}{\tau_4}\right] \right\} \quad (D5)$$

In order to obtain an approximate solution we further assume that  $n_B$  is negligible for  $t < t_d$ , and

$$\frac{Y \dot{D}}{k n_B^0} \gg \frac{1}{\tau_4} \quad (D6)$$

With the above assumptions, we obtain

$$n_B = \frac{P \dot{D} n_B^0}{m Y} \left[ 1 - \exp\left(-\frac{t-t_d}{\tau_4}\right) \right] \quad (D7)$$

Substitution into Eqn. A1 gives

$$\frac{dI_B}{dt} = X \dot{D} P \tau_4 \left[ 1 - \exp\left(-\frac{t-t_d}{\tau_4}\right) \right] \quad (D8)$$

After some substitutions that convert time to dose and consolidate constants this result is equivalent to Eqn. 5 in the text, and is quite consistent with our experimental data.

#### ACKNOWLEDGMENTS

This work was partially supported by the Defense Special Weapons Agency.

#### REFERENCES

- [1] E.W. Enlow, R.L. Pease, W.E. Combs, R.D. Schrimpf, and R.N. Nowlin, "Response of Advanced Bipolar Processes to Ionizing Radiation," *IEEE Trans. Nucl. Sci.*, vol. 38, pp. 1342-1351, Dec. 1991.
- [2] S. McClure, R.L. Pease, W. Will, and G. Perry, "Dependence of Total Dose Response of Bipolar Linear Microcircuits on Applied Dose Rate," *IEEE Trans. Nucl. Sci.*, vol. 41, pp. 2544-2549, Dec. 1994.
- [3] A.H. Johnston, G.M. Swift, and B.G. Rax, "Total Dose Effects on Conventional Bipolar Transistors and Linear Integrated Circuits," *IEEE Trans. Nucl. Sci.*, vol. 41, pp. 2427-2436, Dec. 1994.
- [4] A.H. Johnston, C.I. Lee, B.G. Rax, "Enhanced Damage in Bipolar Devices at Low Dose Rates: Effects at Very Low dose Rates," *IEEE Trans. Nucl. Sci.*, vol. 43, pp. 3049-3059, Dec. 1996.
- [5] Dave Emily, "Total Dose Response of Bipolar Microcircuits," IEEE Nuclear and Space Radiation Effects Short Course, Indian Wells, Ca., 1996, and references therein.
- [6] P. Cole, D. Emily, W. Combs, and R. Pease, "Post-Irradiation Degradation of Input Bias Current on Commercial Linear Circuits," Presented at the IEEE Nuclear and Space Radiation Effects Conference, Indian Wells, Ca., 1996. Some data can be found in the Short Course notes from 1996.

- [7] L. Bonora, and J.P. David, "An Attempt to Define Conservative Conditions for Total Dose Evaluation of Bipolar IC's," *IEEE Trans. Nucl. Sci.*, vol. 44, pp. 1974-1980, Dec. 1997.
- [8] R.K. Freitag and D.B. Brown, "Low Dose Rate Effects on Linear Bipolar IC's: Experiments on the Time Dependence," *IEEE Trans. Nucl. Sci.*, vol. 44, pp. 1906-1913, Dec. 1997.
- [9] D.M. Fleetwood, W.L. Warren, J.R. Schwank, P.S. Winokur, M.R. Shaneyfelt, and L.C. Riewe, "Effects of Interface Traps and Border Traps on MOS Postirradiation Annealing Response," *IEEE Trans. Nucl. Sci.*, vol. 42, pp. 1698-1707, Dec. 1995.
- [10] J.R. Schwank, D.M. Fleetwood, M.R. Shaneyfelt, P.S. Winokur, C.L. Axness, and L. C. Riewe, "Latent Interface-Trap Buildup and its Implications for Hardness Assurance," *IEEE Trans. Nucl. Sci.*, vol. 39, pp. 1953-1963, Dec. 1992.
- [11] D.M. Fleetwood, M.J. Johnson, T.L. Meisenheimer, P.S. Winokur, W.L. Warren, and S.C. Witczak, "1/f Noise, Hydrogen Transport, and Latent Interface Trap Buildup in Irradiated MOS Devices," *IEEE Trans. Nucl. Sci.*, vol. 44, pp. 1810-1817, Dec. 1997.
- [12] R.N. Nowlin, D.M. Fleetwood, R.D. Schrimpf, R. Pease, and W.C. Combs, "Hardness Assurance and Testing Issues for Bipolar/BiCMOS Devices," *IEEE Trans. Nucl. Sci.*, vol. 40, pp. 1686-1693, Dec. 1993.
- [13] D.M. Fleetwood, S.L. Kosier, R.N. Nowlin, R.D. Schrimpf, R.A. Reber, Jr., M. DeLaus, P.S. Winokur, A. Wei, W.E. Combs, and R.L. Pease, "Physical Mechanisms Contributing to Enhanced Bipolar Gain Degradation at Low Dose Rates," *IEEE Trans. Nucl. Sci.*, vol. 41, pp. 1871-1883, Dec. 1994.
- [14] D.M. Fleetwood, L.C. Riewe, J.R. Schwank, S.C. Witczak, and R.D. Schrimpf, "Radiation Effects at Low Fields in Thermal, SIMOX, and Bipolar-Base Oxides," *IEEE Trans. Nucl. Sci.*, vol. 43, pp. 2537-2546, Dec. 1996.
- [15] R.D. Schrimpf, R.J. Graves, D.M. Schmidt, D.M. Fleetwood, R.L. Pease, W.E. Combs, and M. DeLaus, "Hardness-Assurance Issues for Lateral PNP Bipolar Junction Transistors," *IEEE Trans. Nucl. Sci.*, vol. 42, pp. 1641-1649, Dec. 1995.
- [16] S.C. Witczak, R.D. Schrimpf, D.M. Fleetwood, K.F. Galloway, R.C. LaCoe, D.C. Mayer, J.M. Puhl, R.L. Pease, and J.S. Suehle, "Hardness Assurance Testing of Bipolar Junction Transistors at Elevated Irradiation Temperatures," *IEEE Trans. Nucl. Sci.*, vol. 44, pp. 1989-2000, Dec. 1997.
- [17] S.C. Witczak, R.D. Schrimpf, K.F. Galloway, D.M. Fleetwood, R.L. Pease, J.M. Puhl, D.M. Schmidt, W.E. Combs, and J.S. Suehle, "Accelerated Tests for Simulating Low Dose Rate Gain Degradation of Lateral and Substrate PNP Bipolar Junction Transistors," *IEEE Trans. Nucl. Sci.*, vol. 43, pp. 3151-3160, Dec. 1996.